Identification of anti-norovirus genes in mouse and human cells using genome-wide CRISPR activation screening

Authors: Robert C. Orchard[1,2]*, Meagan E. Sullender[1], Bria F. Dunlap[1], Dale R. Balce[1], John G. Doench[3], and Herbert W. Virgin[1]*

Affiliations:

[1]Department of Pathology and Immunology, Washington University School of Medicine, St. Louis, MO 63110

[2] Present address, Department of Immunology, The University of Texas Southwestern Medical Center, Dallas, TX 75390, USA

[3]Broad Institute of MIT and Harvard, Cambridge, MA 02142

[1]Department of Pathology and Immunology, Washington University School of Medicine, St. Louis, MO 63110

Corresponding Authors e-mail: Robert.Orchard@UTSouthwestern.edu (R.C.O); Virgin@wustl.edu (H.W.V.)

16 **Abstract:**

17   Noroviruses (NoVs) are a leading cause of gastroenteritis world-wide, yet host

18 factors that restrict NoV replication are not well understood. Here, we use a CRISPR

19 activation (CRISPRa) genome-wide screening to identify host genes that can inhibit

20 murine norovirus (MNoV) replication in either mouse or human cells. Our screens

21 identified with high confidence 57 genes that can inhibit MNoV infection when

22 overexpressed. A significant number of these genes are in interferon and immune

23 regulation signaling networks, but surprising, the majority of the genes identified are not

24 associated with innate or adaptive immunity nor with any antiviral activity. Confirmatory

25 studies of eight of the genes in validate the initial screening data. Mechanistic studies

26 on *TRIM7* demonstrated a conserved role of the molecule in mouse and human cells in

27 restricting MNoV in a step of infection after viral entry. Furthermore, we demonstrate

28 that two isoforms of *TRIM7* have differential antiviral activity. Taken together these data

29 provide a resource for understanding norovirus biology and demonstrate a robust

30 methodology for identifying new antiviral molecules across cell types and species.

31

32 **Author Summary:**

33   Norovirus is one of the leading causes of foodborne illness world-wide. Despite

34 its prevalence, our understanding of norovirus biology is limited due to the difficulty in

35 growing human norovirus *in vitro* and a lack of an animal model. Murine norovirus

36 (MNoV) is a model norovirus system because MNoV replicates robustly in cell culture

37 and in mice. To identify host genes that can restrict norovirus replication when

38 overexpressed we performed genome-wide CRISPR activation (CRISPRa) screens to

39 induce gene overexpression at the native locus through recruitment of transcriptional

40 activators to individual gene promoters. We found 57 genes could block murine

41 norovirus replication in either mouse or human cells. Several of these genes are

42 associated with classical immune signaling pathways, while many of the molecules we

43 identified have not been previously associated with antiviral activity. Our data is a

44 resource for those studying norovirus and we provide a robust approach to identify

45 novel antiviral genes.

46

Introduction:

Noroviruses are non-enveloped viruses with positive-sense RNA genomes that infect the gastrointestinal tract of mammals [1]. Human norovirus (HNoV) is the leading cause of viral gastroenteritis worldwide and is estimated to have an economic burden of $1 billion annually [2]. Despite the high infectivity of HNoV between individuals, it has proven difficult to culture *in vitro* with significant advances made only in the past few years [3, 4]. Because of the challenges in growing HNoV in cell culture and lack of an animal model, murine norovirus (MNoV) has emerged as a system for understanding norovirus biology. MNoV grows robustly in cell culture, is amenable to reverse genetics, and is a natural pathogen of laboratory mice. MNoV is similar to HNoV in that both viruses are spread fecal-orally, infect intestinal tissues, have similar genomic organization and protein function, and can establish persistent infection in individuals [1].

Host factors that limit or modulate norovirus replication are still not well understood. We and others previously used a whole-genome CRISPR/Cas9 loss-of-function screen to identify essential host factors required for MNoV growth in macrophage-like cell lines leading to the identification of CD300lf as a proteinaceous receptor for MNoV [5, 6]. Importantly, expression of mouse CD300lf in cells is sufficient for replication in all cell types tested including human cells, thus expanding the repertoire of cell lines that can be utilized to study norovirus infection with MNoV [5, 6]. These studies also demonstrate that the cellular machinery for replication of MNoV is highly conserved with species specificity conferred by the receptor. While CRISPR knockout studies for MNoV and other viruses have identified host factors necessary for

4

70   viral infection, they have yet to identify restriction factors that antagonize viral replication

71   [5-11].   Recent modifications of the CRISPR/Cas9 system has led to the ability to

72   transactivate gene expression through specific recruitment of transcriptional activators

73   to individual promoters and has been broadly called CRISPR activation (CRISPRa; [12-

74   14]). cDNA overexpression systems have been used to identify viral restriction factors

75   but this approach has several technical hurdles, most notably the cloning, delivery, and

76   expression of large transcripts and the need to select individual protein isoforms rather

77   than screening for the effects of all transcripts that emanate from a given cellular gene

78   promoter. Because CRISPRa induces gene expression from the native locus and relies

79   only on sgRNA homology for specificity, it overcomes many of these obstacles. We

80   therefore utilized CRISPRa to identify genes whose overexpression block MNoV

81   replication.

82   We use recently developed CRISPRa genome-wide libraries to screen for host

83   genes that antagonize MNoV replication in both mouse and human cells. Our screens

84   and subsequent validation identify numerous anti-MNoV genes including canonical

85   interferon stimulated genes and several genes with novel antiviral activity.   We

86   demonstrate that the antiviral activity of one such gene, *TRIM7*, is highly specific to only

87   one of the two major *TRIM7* isoforms, highlighting the utility and power of the CRISPRa

88   screening approach.   Further mechanistic studies demonstrate that TRIM7 inhibits

89   MNoV replication post viral entry. These data provide a resource for understanding

90   norovirus biology and a methodology for identifying unappreciated viral restriction

91   factors.

92

Results:

Generation of CRISPRa libraries in mouse and human cells

93

94

95　　　　We set out to identify genes in mouse and human cells that have anti-norovirus

96　activity when overexpressed. By screening cell lines from two different species, we

97　sought to capture a wider diversity of antiviral genes and potentially identify those

98　molecules with evolutionary conserved antiviral function. We first generated cell lines

99　that can be infected by MNoV and express the CRISPRa machinery. For the mouse

100　screen, we used BV2 microglial cells, previously used for loss-of-function CRISPR

101　screening, in which MNoV replicates robustly [5]. As noroviruses exhibit strict species

102　tropism and at this time HNoV replication is not robust or scalable for whole-genomic

103　pooled screens, we selected HeLa cells to use as a model human cell line and

104　generated HeLa-CD300lf stable cells that can be infected by MNoV. We introduced the

105　catalytically dead Cas9-VP64 (dCas9-VP64) fusion construct into both the BV2 and

106　HeLa-CD300lf cell lines (BV2-dCas9-VP64 and HeLa-CD300lf-dCas9-VP64).

107　　　　Before proceeding with a genome-wide screen, we developed a simple assay to

108　test transcriptional activation activity in BV2-dCas9-VP64 and HeLa-CD300lf-dCas9-

109　VP64 cells relying on the low level of expression of CD4 in these cells. sgRNAs

110　targeting the CD4 transcriptional start site robustly increased the surface levels of CD4

111　in BV2-dCas9-VP64 and HeLa-CD300lf-dCas9-VP64 cells compared to an empty

112　vector control (Figure 1A-1B).

113　　　　We next introduced a pooled, genome-wide CRISPRa library into BV2-dCas9-

114　VP64 (Caprano library) and HeLa-CD300lf-dCas9-VP64 (Calabrese library) cells.

115　Importantly, these libraries use an updated CRISPRa sgRNA vector system (Sanson et

6

116   al. in preparation). This system (pXPR_502) is bicistronic with one promoter expressing

117   the sgRNAs with PP7 stem loops while the second promoter drives expression of the

118   synergistic transcriptional activators (Figure 1A). This new system is advantageous

119   over the previous synergistic activation mediator (SAM) vectors as it consolidates the

120   transcription activators and sgRNA into one lentivirus [14]. Caprano and Calabrese

121   libraries contain 134,076 and 113,240 total sgRNAs, respectively, with each gene

122   targeted with 3-6 sgRNAs split between two pools, SetA and SetB. After introduction of

123   these libraries into BV2-dCas9-VP64 and HeLa-CD300lf-dCas9-VP64 cells, we

124   challenged the resulting pools with either MNoV[CW3] and MNoV[CR6] and isolated resistant

125   cells (Figure 1D). MNoV[CW3] causes acute, systemic infection in mice while MNoV[CR6]

126   establishes a persistent infection in intestinal tuft cells, a specialized intestinal epithelial

127   cell [15-17]. MNoV[CW3] and MNoV[CR6] have been used to model human noroviruses,

128   transkingdom interactions, and innate immunity restriction of viral tropism [4, 18-23]. In

129   summary, we performed four independent CRISPRa screens using two different cell

130   lines (BV2 vs. HeLa) and two different viral strains (MNoV[CW3] and MNoV[CR6]) in an effort

131   to provide a broad resource for understanding norovirus biology in multiple cellular

132   settings.

133

134   **CRISPRa screen for anti-MNoV in BV2 cells**

135   BV2-dCas9-VP64 cellular pools containing the Caprano library were infected with

136   MNoV[CW3] or MNoV[CR6] at an MOI of 5. Surviving cells were harvested after a brief

137   expansion period (Figure 1D). sgRNAs from resistant cells were compared to mock

138   infected control using STARS (Doench et al., 2016). The STARS algorithm calculates a

139 score and a false discovery rate (FDR) for a gene with at least two sgRNAs enriched in

140 the top 10% of a ranked ordered list of total sequenced sgRNAs. We consider a gene a

141 hit in an individual screen if the FDR was < 0.25. Five and seven genes met this

142 criterion in BV2 cells that survived MNoV^{CW3} or MNoV^{CR6} infection, respectively. Four

143 genes (*Trim7*, *Prdm1*, *Tbx19*, and *Obox6*) were enriched after challenge with both viral

144 strains (Tables S1-S2 and Figure 2A-2B). Gene Set Enrichment Analysis (GSEA) of the

145 screen hits demonstrated an enrichment in interferon gamma and alpha response

146 pathways, consistent with the known role of these responses to limit viral replication

147 (Table 1). Overall these results demonstrate the ability of the CRISPRa technology in

148 identifying antiviral activity of overexpressed genes.

149

150 **CRISPRa screen for anti-MNoV genes in HeLa-CD300lf cells**

151 In comparison to BV2 cells, MNoV exhibits less selective pressure in HeLa-

152 CD300lf cells and thus an MOI of 50 for MNoV^{CW3} and MNoV^{CR6} was used, additionally,

153 a second challenge of MNoV^{CR6} was preformed to exert a high selective pressure for

154 this strain of virus (see methods for more details). sgRNAs were sequenced from

155 resistant cells and compared to a mock infected control using the STARS algorithm [24].

156 33 and 22 genes in MNoV^{CW3} and MNoV^{CR6} infected HeLa-CD300lf, respectively,

157 scored as hits (Tables S3-S4 and Figure 2A and 2C). Six genes (*TRIM7, PITX1,*

158 *HOXC11, DDX60, MX1, and PLSCR1*) were enriched after challenge with both viruses.

159 To explore the possibility that individual hits function in a similar pathway, we

160 took the 49 genes that scored for either viral strains and analyzed them using GSEA

161 [25, 26]. Comparison of the hallmark genes with our dataset indicated a significant

8

162 enrichment in genes related to interferon alpha responses, including *GBP2*, which has

163 been recently shown to block MNoV replication complex formation [27]. When

164 analyzing the function of the genes by GO terms we also found an enrichment for

165 interferon and cytokine responses along with genes involved in embryogenesis and

166 RNA polymerase gene expression (Table 2). These data demonstrate the ability to

167 discover expected candidate antiviral genes (e.g. those regulated by inflammatory

168 cytokines) and candidate genes involved in other pathways (e.g. embryogenesis).

169

170 **Analysis and comparison of screen in BV2 and HeLa cells**

171 We compared the results from the BV2 and HeLa-CD300lf CRISPRa screens.

172 The top hit in all virus and cell type combinations was *TRIM7* (Figure 2A and Tables S1-

173 S4). No other gene had an FDR <0.25 and only *TRIM7* and *PLSCR1* had a STARS

174 score > 2.0 in all four screens (Figure 2A). Similar results are obtained when we

175 subdivide the screens based upon viral strain (Tables S1-S4). When looking at the

176 GSEA both screens had an interferon signature (Table 1 and 2). The lack of

177 concordance between other hits could be due to cell type, species, library, or selective

178 pressure differences between screens. Additionally, we find that false-negatives are

179 common (see below) and our data likely underrepresents the true overlap of function

180 across the cellular systems. None the less, these data highlight the importance of

181 examining multiple cell types for antiviral genes.

182

183 **Validation of CRISPRa screening results in HeLa cells**

184 　　　　We validated our screening results in human cells. We individually, introduced 2

185 sgRNAs per gene into HeLa-CD300lf-dCas9-VP64 cells targeting *TRIM7*, *MUC1*,

186 *LRRC15*, *PLSCR1*, *HOXC11*, *GBP2*, *MX1*, *BLNK* and compared to cells transduced

187 with an empty pXPR_502 vector or pXPR_502 with a sgRNA targeting CD45. These

188 genes encompass seven of the top 15 enriched genes after MNoV^{CW3} challenge.

189 Additionally, three of the eight genes showed enrichment in an MNoV-strain dependent

190 manner (MUC1 and GBP2 for MNoV^{CW3} and BLNK for MNoV^{CR6}) and thus were ideal

191 for testing strain specificity for potentially antiviral molecules.

192 　　　　As the screen was designed to enrich for genes that protected cells from virus

193 induced cytopathic effect (CPE), we first tested the ability of cells to survive MNoV

194 infection. All genes tested had at least one sgRNA show statistical growth advantage

195 over control cells when challenged with either MNoV^{CW3} or MNoV^{CR6} (Figure 3A and

196 3B). Furthermore, four of the eight and five of the eight genes had both sgRNAs

197 provide a survival phenotype when challenged with MNoV^{CW3} and MNoV^{CR6},

198 respectively (Figure 3A and 3B). We were unable to validate an MNoV strain-specific

199 protective effect for any gene (Figure 3C). Taken together, these data validate the

200 reproducibility of the CRISPRa screening platform and indicate the potential for false-

201 negatives.

202 　　　　We next tested whether overexpression of these genes inhibited production of

203 infectious virions by analyzing the amount of MNoV replication 24 hours-post infection

204 (Figure 3D and 3E). Six of the eight (MNoV^{CW3}) five of the eight (MNoV^{CR6}) genes

205 tested had at least one sgRNA significantly reduce the amount of MNoV produced

206 (Figure 3D-3F). Additionally, both sgRNAs for three genes (*TRIM7*, *GBP2*, and *MX1*)

207   blocked the production of MNoV^{CW3} and MNoV^{CR6}. In summary these data provide the

208   first systematic overview of the molecules that can inhibit MNoV infection in human

209   cells.

210

211   Isoform specificity of the antiviral activity of TRIM7

212   While we have identified a significant number of novel antiviral molecules, our

213   overarching goal is to identify molecules that broadly inhibit NoV replication in multiple

214   cellular contexts. Given that the top gene in all four screens was *TRIM7*, we decided to

215   focus our efforts on characterizing the anti-MNoV activity of *TRIM7* in HeLa and BV2

216   cells. TRIM7 (also GNIP) is an E3-ligase previously shown to interact with glycogenin

217   and ubiquitinate the AP-1 coactivator RACO1; however the role of TRIM7 during viral

218   infection has not been explored [28, 29].

219   TRIM7 has at least 4 isoforms in humans with isoform 1 and isoform 4 being the

220   most commonly studied and display different expression pattern in muscular tissues and

221   cells [30]. We generated stable BV2 and HeLa-CD300lf cells overexpressing human

222   TRIM7 isoform 1 or isoform 4 (Figure 4A). While expression of TRIM7 isoform 1

223   protected both HeLa-CD300lf and BV2 cells from MNoV CPE, TRIM7 isoform 4

224   provided no protection (Figure 4B-4E). TRIM7 isoform 1, but not isoform 4, reduced the

225   growth of MNoV^{CW3} and MNoV^{CR6} in both human and mouse cells (Figure 4F-4I). Taken

226   together, these data demonstrate an isoform specificity for the anti-MNoV mechanism

227   that is conserved across species.

228   Finally, we determined which step of the viral life cycle was targeted by TRIM7.

229   Since ubiquitination can lead to proteaseome-mediated degradation of proteins, we first

230   tested whether the MNoV receptor, CD300lf, was reduced upon TRIM7 overexpression.

231   In HeLa-CD300lf we found no effect of TRIM7 on CD300lf protein levels (Figure 4A).

232   We next tested the hypothesis that TRIM7 targets a critical step of MNoV entry.

233   Transfection of MNoV^{CW3} RNA was unable to rescue MNoV production in human TRIM7

234   isoform 1 expressing BV2 cells indicating that TRIM7 can target a post-entry step of the

235   MNoV life cycle to inhibit viral replication (Figure 4J).

236

237   **Discussion:**

238   Here we present a genome-wide screen to identify genes that can inhibit murine

239   norovirus replication upon overexpression in both mouse and human cells. Our results

240   provide a resource for those studying norovirus biology and validate CRISPRa

241   screening as an approach to uncover novel antiviral molecules. As human norovirus

242   studies are limited due to the difficulty in culturing the virus in cell culture, we speculate

243   that our screens with MNoV in mouse and human cells may identify evolutionary

244   conserved genes that may broadly inhibit NoV replication. Such genes might be

245   targeted through genetic or chemical perturbagens to enhance HNoV replication in cell

246   culture systems, or to generate therapeutic effects.

247   With the discovery that Cas9 binding to DNA does not require nuclease activity,

248   several new technologies have emerged to synthetically modulate mammalian genomes

249   with unprecedented precision and scale [31]. By leveraging the cytotoxicity of lytic

250   viruses, these pooled screening approaches are ideal to identify genes that alter viral

251   infection. While most investigations using CRISPR/Cas9 genome-wide screens have

252 focused on determining host factors that facilitate viral infection, our results highlight the

253 utility of CRISPRa to identify antiviral molecules.

254   Genes identified in these screens exhibited enrichment in viral and immune

255 related genes not previously appreciated to have anti-MNoV activity (Figure 2A). Given

256 that the tropism of both acute and persistent strains of MNoV are dictated by

257 interferons, these data provide the first insight into potential interferon stimulated genes

258 (ISGs) that mediate viral restriction of MNoV [18, 19, 21]. It will be important to

259 determine whether these ISGs contribute to determining norovirus tropism *in vivo*.

260   Surprisingly, in addition to the ISGs, a number of genes not appreciated to have

261 immune functions were identified as possessing anti-MNoV activity (Figure 2A). These

262 represent unique opportunities to identify novel norovirus vulnerabilities and to

263 determine whether these genes possess antiviral activity against other viruses that may

264 explain tropism or be exploited for therapeutic potential. One of these genes, TRIM7,

265 inhibited MNoV replication after viral entry (Figure 4I). As ubiquitination can have

266 diverse effects on protein stability and function, it will be essential to determine the

267 substrate and type of lysine-linkage in order to understand the mechanism of viral

268 restriction [32]. Additionally, we mapped the antiviral function of TRIM7 to a specific

269 isoform, while a closely related isoform had no detectable anti-MNoV activity (Figure

270 4A-4H). The only differences between these isoforms are within the protein-protein

271 interaction coiled-coil domain SPRY domains. As these molecules can be differentially

272 and coexpressed in different cellular contexts and TRIM proteins are capable of

273 homodimerization, it will be important to determine if isoform 4 can regulate the antiviral

274 activity or the normal physiological functions of isoform1 [33].   Furthermore, as

13

275   traditional cDNA based screens require the scientist to select a specific isoform,

276   CRISPRa approaches enable complex transcriptional variance to be reduced and

277   encompassed by sgRNAs, which is highlighted by the specificity of anti-MNoV by

278   TRIM7 isoforms [14].

279   In conclusion, our data provides the first systematic insight into genes that can

280   restrict norovirus replication when overexpressed and provides a methodological

281   approach to identify novel antiviral molecules using CRISPRa technology that may be

282   broadly applicable to other viral systems.

283

284 **Methods**

285 Cell culture

286 BV2 cells (BV-2 cells were provided by Dr. Yuanan Lu, University of Hawaii at Manoa),

287 293T (ATCC) and Hela cells (ATCC) were cultured in Dulbecco's Modified Eagle

288 Medium (DMEM) with 10% fetal bovine serum (FBS), and 1% HEPES. HeLa cells were

289 transduced with pCDH-MSCV-CD300lf-T2A-Hygromycin and selected with Hygromycin

290 for 2 weeks prior to sorting CD300lf high expressing cells to generate HeLa-CD300lf-

291 Hygromycin cells. For BV2 cells, 4 µg/ml of puromycin (Sigma Aldrich) and 5 µg/ml

292 blasticidin (Invitrogen), was added where appropriate. For HeLa cells, 1 µg/ml of

293 puromycin, 5 µg/ml blasticidin, and 350 µg/ml hygromycin (Invitrogen) were added as

294 appropriate.

295 Lentivirus was generated by transfecting lentiviral vectors with packaging vector

296 (psPAX2) and pseudo-typing vector (pCMV-VSV-G) into 293Ts using TransIT-LT1

297 (Mirus). 48 hours post-transfection, supernatants were collected, filtered through a 0.45

298 µm filter (Millipore), and added to the indicated cells. After 48 hours, cells were selected

299 with the appropriate antibiotic.

300

301 Plasmids

302 Guide constructs were cloned into pxpr_502 (Addgene #96923). A complete list

303 of guide sequences used in this study can be found in the supplemental materials.

304 Human *TRIM7* isoform 1 (NP_976038.1) and isoform 4 (NP_203128.1) were codon

305 optimized and cloned into pCDH-MCS-T2A-Puro-MSCV (Systems Biosciences #

15

306   CD522A-1). Codon optimized cDNA sequences for the constructs can be found in the

307   supplemental materials. All plasmids were sequenced verified prior to use.

308

309   Transcriptional Activation Reporter Assays

310   BV2 cells and HeLa-CD300lf cells were transduced with pLenti-dCas9-VP64-

311   Blast [14]. Transcriptional activity was assessed in these cells by transducing either

312   parental or dCas9-VP64 cells with pxpr_502 lentiviruses targeting CD4. Cells were

313   transduced for 2 days and subsequently, selected for 7 days with puromycin and the

314   frequency of CD4 expression was assessed by flow cytometry.

315

316   BV2 CRISPRa screen

317   BV2-dCas9-VP64 cells were transduced with Set A and SetB of the caprano

318   CRISPRa library at an MOI of 0.3 to 0.5 (Sanson et al. in preparation). Transductions

319   were performed with enough cells to enable each sgRNA in the library to be

320   represented at least 500 times. Each experimental condition was performed in

321   duplicate with each replicate consisting of 3.0×10^7 BV2 cells expressing the complete

322   CRISPRa system seeded equally across three 150cm2 dishes on day five post-

323   transduction. Cells were infected 24 hours later with either MNoV^{CW3} or MNoV^{CR6} at

324   MOI of 5. Mock infected cells were harvested 48 hours after seeding. Ten days post-

325   infection surviving cells were harvested. Genomic DNA was isolated from cells using

326   Mini ($<5 \times 10^6$ cells), Midi (5×10^6 - 3×10^7 cells), and Maxi (3×10^7 cells - 1×10^8

327   cells), kits (Qiagen) according to the Broad Institute's Genetic Perturbation Platform

328   protocols (https://portals.broadinstitute.org/gpp/public/resources/protocols).

16

329

330   HeLa CRISPRa screen

331   HeLa-CD300lf cells expressing dCas9-VP64 were transduced with the Set A and

332   SetB of the caprano CRISPRa library at an MOI of 0.3.   Each Calabrese pool was

333   delivered by lentiviral transduction of 1.2×10^8 HeLa cells at an MOI ~0.3. This equates

334   to 3.6×10^7 transduced cells, which is sufficient for the integration of each sgRNA at

335   least 500 independent times. Two days post transduction, puromycin was added to the

336   media and transduced cells were selected for a total of 7 days. 5×10^6 HeLa CRISPRa

337   cells were seeded in a T175 tissue culture flask and for each experimental conditional

338   was done in duplicate with 6 independent flasks per replicate (3e7 cells per replicate).

339   Cells were infected with either MNoV^{CW3} or MNoV^{CR6} at an MOI 50 at the time of

340   seeding. Two days after infection, mock infected cells were harvested for genomic DNA

341   extraction.   At this time point, roughly 85% of the MNoV^{CW3} infected cells displayed

342   cytopathic effect while MNoV^{CR6} cells had 35-50% and both sets of conditions had cells

343   washed twice with PBS and fresh media added.   After an additional 2 days of viral

344   challenge MNoV^{CR6} challenged cells had roughly 25% viable cells and thus were

345   washed, trypsinized, collected and counted and replated at 5×10^6 cells/flask and

346   rechallenged. The MNoV^{CW3} challenged cells had <10% viable at this time point and

347   thus only a single challenge was performed.   Cells were harvested after the second

348   challenge of MNoV^{CR6} and the single challenge of MNoV^{CW3} when they started to form

349   discernable, stable colonies, between 7-14 days from the initial challenge.   All flasks

350   from a single replicate were harvested together.   Genomic DNA was isolated from

351 surviving cells using a Qiamp DNA mini kit according to manufacturer instructions

352 (Qiagen).

353

354 CRISPR screen sequencing and analysis

355   Illumina sequencing and STARS analysis was performed as described previously

356 [5]. Briefly, genomic DNA was aliquoted into multiple wells of a 96-well plate with up to

357 10 μg of DNA in 50 μl total volume. A PCR mastermix consisting of ExTaq DNA

358 polymerase (Clontech), ExTaq buffer, dNTP, P5 stagger primer, and water was

359 generated. 40 μl of PCR master mix, and 10 μl of a barcoded primer was added to each

360 well containing 50 μl of DNA. Samples were PCR amplified as follows: 95°C for 1min.,

361 followed by 28 cycles of 94°C for 30 sec., 52.5°C for 30sec., 72°C for 30 sec. with a

362 final 10 min. at 72°C. PCR product was purified with Agencourt AMPure XP SPRI beads

363 according to the manufacture's protocol (Beckman Coluter). Samples were sequenced

364 on an Illumina HiSeq 2000. Barcodes in the P7 primer were deconvuluted and the

365 sgRNA sequence was mapped to a reference file of sgRNAs in the caprano or

366 calabrese library. To normalize for different numbers of reads per condition, read counts

367 per sgRNA were normalized to 10^7 total reads per sample. This normalized value was

368 then log-2 transformed. sgRNAs that were not sequenced were arbitrarily assigned a

369 read count of 1. Replicates were then averaged together and sgRNA frequencies were

370 then analyzed using STARS software, which is available at

371 http://www.broadinstitute.org/rnai/public/software/index [24]. STARS computes a score

372 for each gene of rank-ordered sgRNA hits that was above 10% of total sequenced

373   sgRNAs. A STAR score was assigned to genes that had a sgRNA score above this

374   threshold in either of the two independent pools.

375   For GSEA analysis, screen hits were queried at the BROAD GSEA portal

376   (https://software.broadinstitute.org/gsea/index.jsp). Only the top 20 gene set names

377   with an FDR < 0.05 are shown in the tables.

378

379   MNoV Assays

380   MNoV^{CW3} (Gen bank accession no. EF014462.1) and MNoV^{CR6} (Gen bank

381   accession no. JQ237823) were generated by transfecting MNoV cDNA clones into 293T

382   cells as described previously [16]. For cell survival assays, 1 x 10^4 of the indicated

383   HeLa cells were seeded in wells of a white-walled 96-well plate (Corning) with indicated

384   MNoV strains at an MOI of 50. 72 hours post-infection, viability was measured using

385   CellTiter-Glo (promega) following manufactures protocol. Viability for each cell line was

386   normalized to a mock infected sample. Each condition was performed at least in

387   triplicate in three independent experiments. A similar experimental set up was

388   performed for BV2 cells except an MOI of 5.0 was used and viability was assessed after

389   24 hours of infection.

390   For MNoV growth curves, 5 x 10^4 cells infected in suspension with MNoV^{CW3} or

391   MNoV^{CR6} at an MOI of 0.05 in a well of a 96-well plate. Plates were frozen at 12 or 24

392   hours post infection at -80ºC for BV2 and HeLa cells, respectively. Total cell lysate was

393   used in subsequent plaque assays as previously described [34]. All infections were

394   done in triplicate in each of at least three independent experiments.

395   Viral RNA (vRNA) from MNoV^{CW3} was extracted from cell-free viral preparations

396   using TRIzol (Invitrogen) according to manufacturer instructions. Purified vRNA was

397   plaqued to ensure complete inactivation of MNoV. 4 μg of vRNA was transfected into

398   BV2 cells using Lipofectamine 2000 (Invitrogen) according to the manufacturer's

399   protocol. Transfected cells were frozen 12 hours later. Each condition was assayed by

400   plaque assay in duplicate in three independent experiments.

401

402   Antibodies and Western Blotting

403   The following antiboides were used for flow cytometry or western blotting as

404   indicated: rabbit α-TRIM7 (Sigma) mouse α-GAPDH-HRP (Sigma), armenian hamster

405   α-CD300lf clone 3F6 (Genentech) anti-human CD4 (Invitrogen; clone S3.5), and anti-

406   mouse CD4 (Biolegend; clone RM4-5).

407   Cells were placed on ice, washed once in PBS, prior to lysis in cold RIPA Buffer (

408   50 mM Tris pH 7.4, 150 mM NaCl, 2 mM EDTA, 1% IGEPAL, 0.5% Sodium

409   Deoxycholate, and 0.1% SDS) with HALT protease and phosphastase inhibitor cocktail

410   (Sigma). Lysates were clarified by centrifugation prior to resolving on SDS-PAGE gels

411   (BioRad) and transfer to PVDF membranes.

412

413   Data availability

414   The data that support the findings of this study are available from the corresponding

415   authors upon request.

416

417   **Acknowledgements**

Figure 1

A

B

C

D

418   We   would   like   to   thank

419   Megan   Baldridge   and   Craig

420   Wilen   for   helpful

421   conversations   and

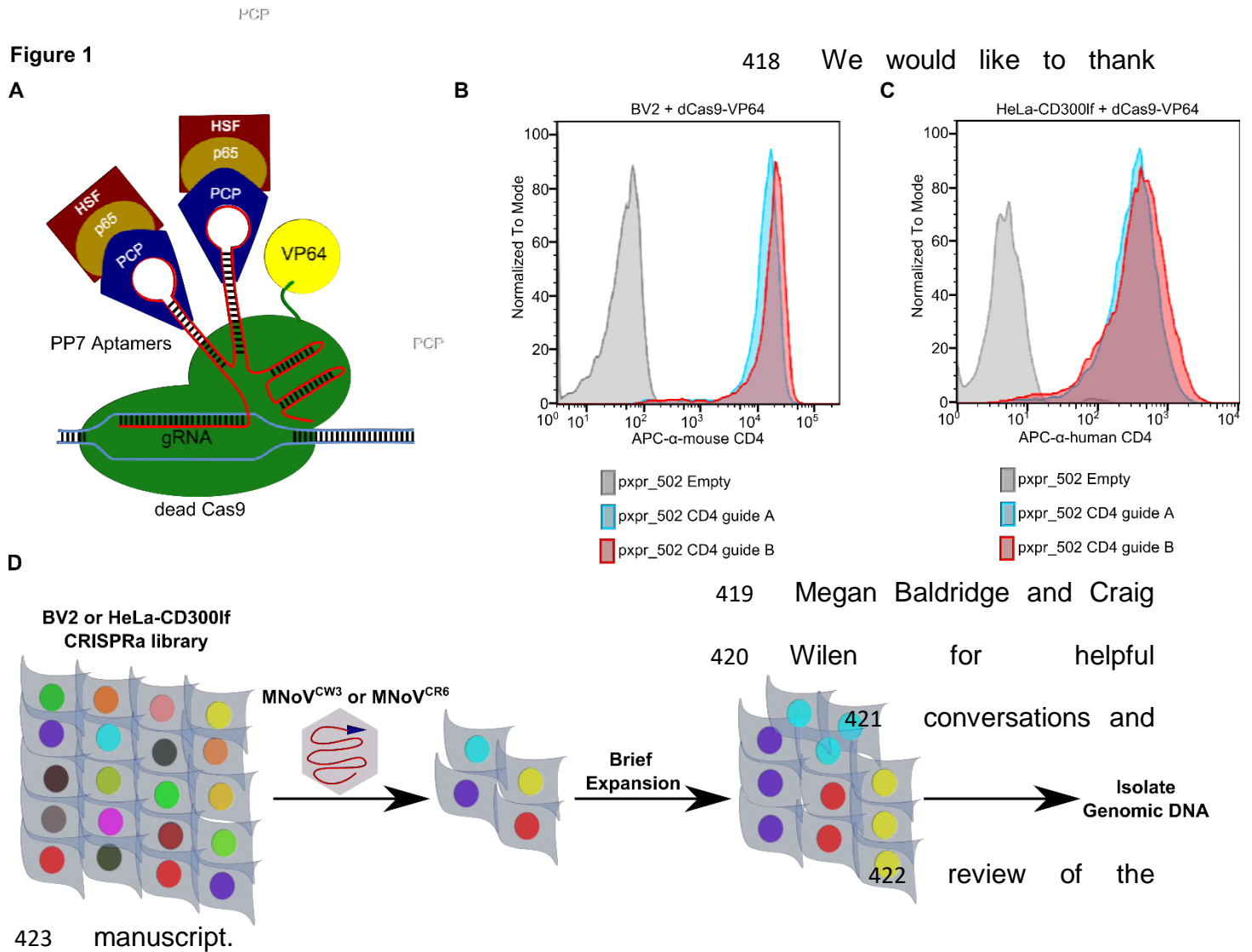422   review   of   the

423   manuscript.

424

425

426

427

428 **Figure 1: CRISPRa screen for anti-norovirus genes**

429 **(A)** Schematic of the CRISPRa system used in this study. Dead Cas9 (dCas9) fused to

430 VP64 interacts with sgRNAs at the transcriptional start site of a gene. sgRNA have PP7

431 hairpins that recruit a chimeric protein containing Heat Shock Factor (HSF), p65

432 transcription factor, and phage coat protein (PCP) fused together. In combination this

433 leads to the transcriptional activation of the targeted gene.

434 **(B-C)** BV2 **(B)** or HeLa-CD300lf **(C)** expressing dead Cas9-VP64 fusion were

435 transduced with the indicated sgRNA plasmids and assayed for CD4 expression one

436 week after antibiotic selection. At base line CD4 levels are low but dramatically

437 increase upon expression of the CRISPRa machinery being present.

438 **(D)** Cartoon overview of the cell survival CRISPRa screen performed with BV2 and

439 HeLa-CD300lf cells. sgRNAs from cells surviving MNoV challenge were analyzed and

440 compared to relative abundance of a mock infected sample.
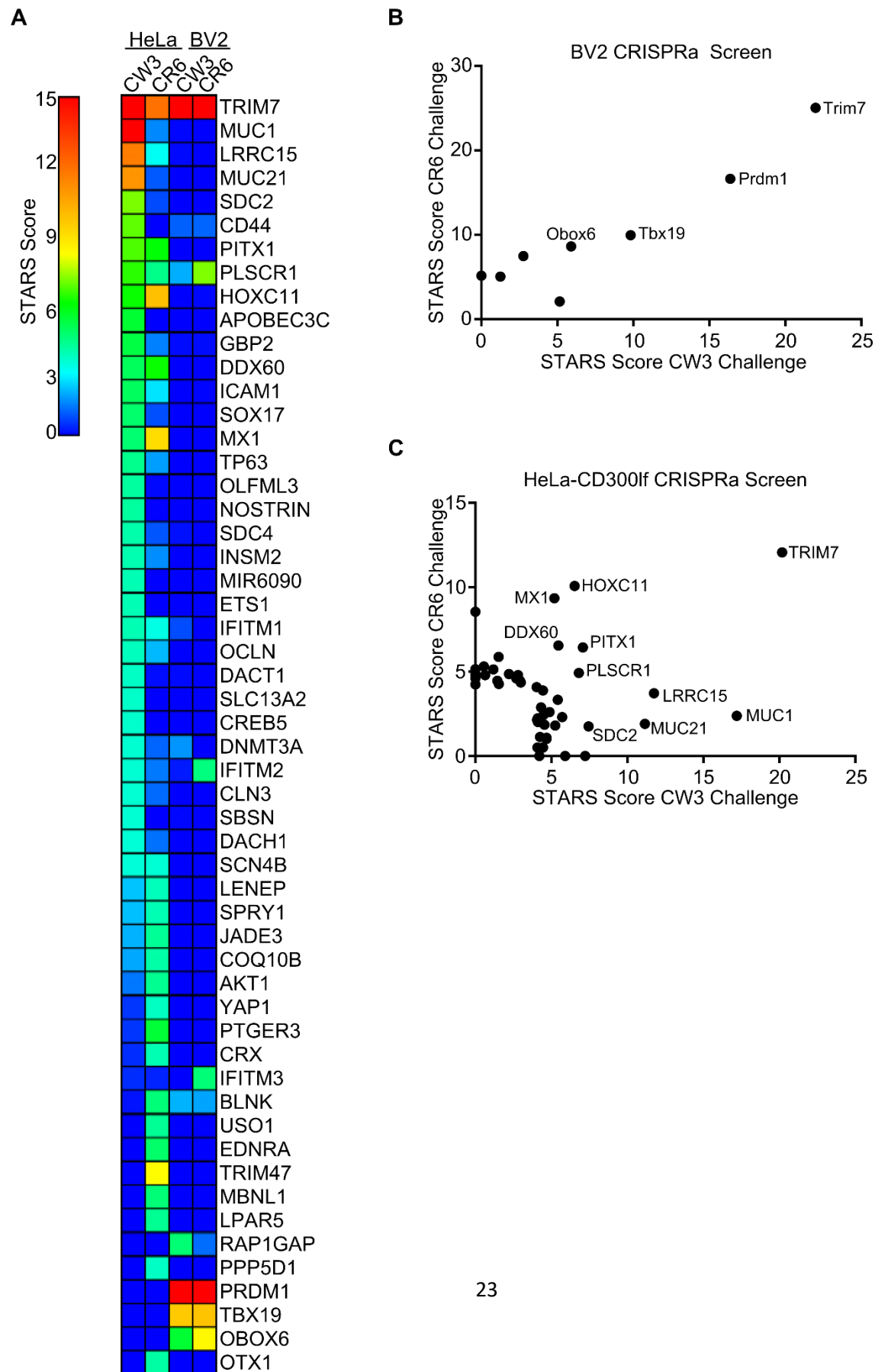
441

Figure 2 442

Figure 2: Identification of anti-MNoV genes in mouse and human cells

(A) A heat map showing enrichment of genes in the four indicated conditions. Genes are color coded based upon their STARS score.

(B) A comparison of the STARS score from BV2 cells challenged with MNoV^{CW3} (x-axis) and MNoV^{CR6} (y-axis). Genes that did not meet the criteria to receive a STARS score are assigned a value of 0.

(C) A comparison of the STARS score from HeLa-CD300lf cells challenged with MNoV^{CW3} (x-axis) and MNoV^{CR6} (y-axis). Genes that did not meet the criteria to receive a STARS score are assigned a value of 0.
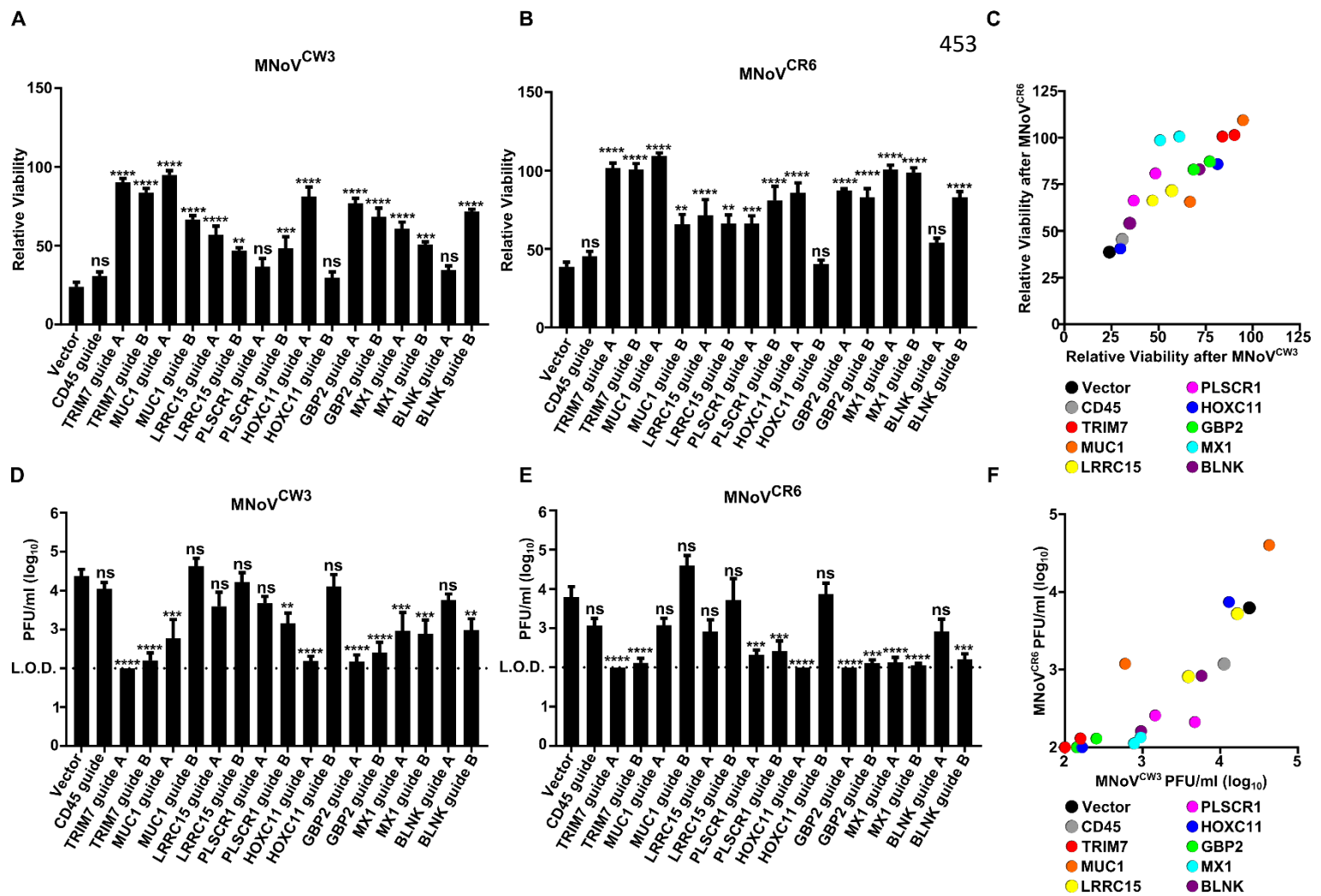
Figure 3

453

Figure 3: Validation of anti-MNoV genes in human cells

(A-B) HeLa-CD300lf cells expressing dCas9-VP64 and the indicated sgRNAs were challenged with MNoVCW3 **(A)** or MNoVCR6 **(B)** at an multiplicity of infection (MOI) of 50. Cellular viability was assessed 72 hours post infection (hpi). Values are normalized for each cell line to uninfected control wells to determine % viability. Data are shown as means ± SEM from three independent experiments and data were analyzed by one-way ANOVA with Tukey's multiple comparison test. *p<0.05, **p<0.01, ***p<0.001, ****p<0.0001, ns = not significant.

(C) A graph depicting the correlation between the relative viability of cell lines after 72 hours of MNoV^{CW3} (x-axis) and MNoV^{CR6} (y-axis) infection. Each dot represents the average relative viability over three independent experiments that the indicated sgRNA expressing cell line exhibited.

(D-E) HeLa-CD300lf cells expressing dCas9-VP64 and the indicated sgRNAs were infected with MNoVCW3 **(D)** or MNoVCR6 **(E)** at an MOI of 0.05. Viral production was assessed 24 hpi as measured by plaque assay. Data are shown as means ± SEM from three independent experiments and data were analyzed by one-way ANOVA with Tukey's multiple comparison test. *p<0.05, **p<0.01, ***p<0.001, ****p<0.0001, ns = not significant.

(F) A graph depicting the correlation between the viral production 24 hours after MNoV^{CW3} (x-axis) and MNoV^{CR6} (y-axis) infection. Each dot represents the average plaque forming units (PFU)/ml over three independent experiments that the indicated sgRNA expressing cell line exhibited.
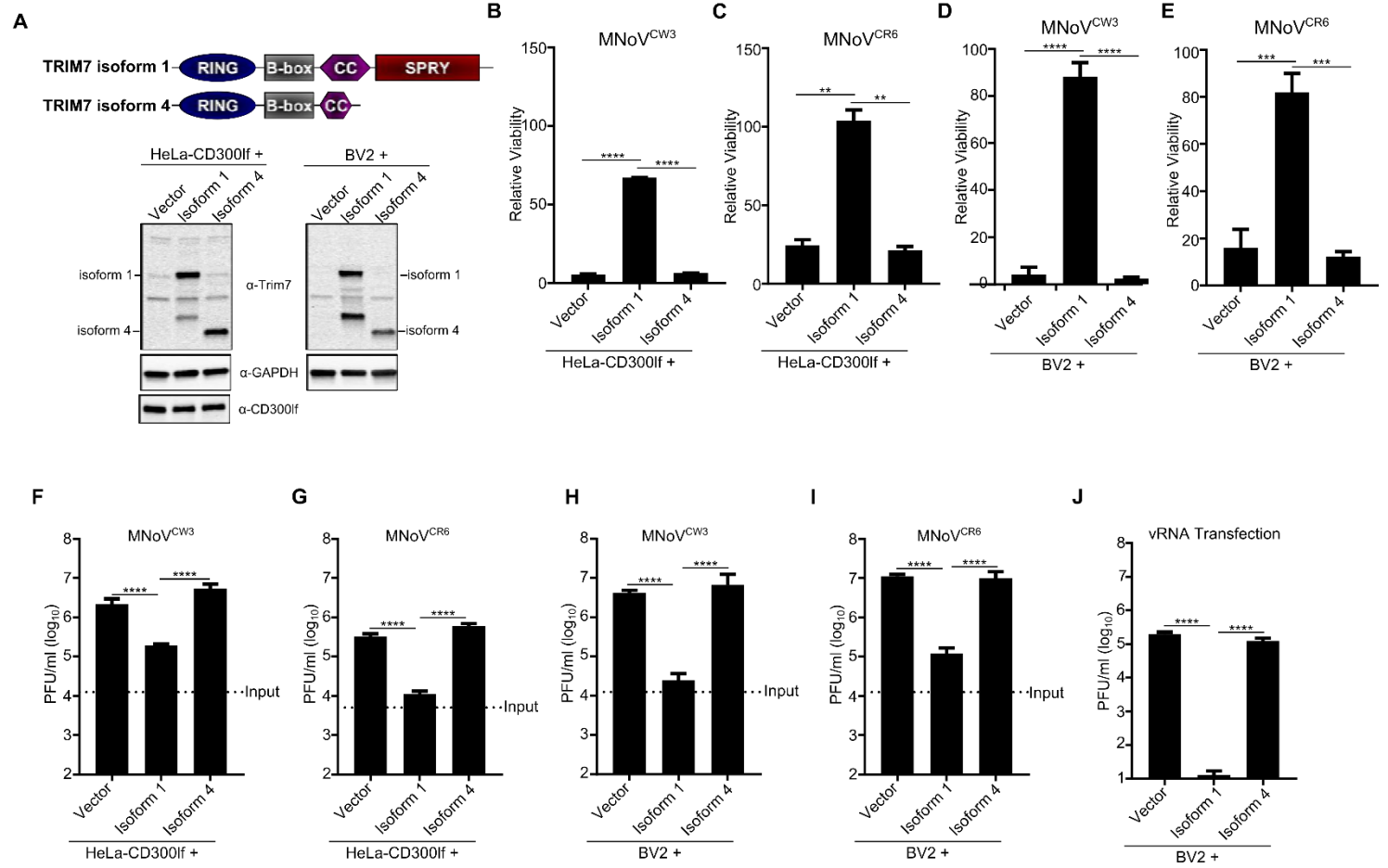
Figure 4

477

27

478 **Figure 4: A specific TRIM7 isoform inhibits MNoV replication post-entry**

479 **(A)** (Top) Cartoon diagram of TRIM7 isoform 1 and isoform 4. RING, B-box, coiled-coil

480 (CC) and SPRY domains are displayed. Isoform 4 has an alternative, shorter coiled coil

481 domain and does not encode a SPRY domain. (Bottom) Representative western blot

482 for indicated protein expression in BV2 or HeLa-CD300lf cells expressing either an

483 empty vector, TRIM7 isoform 1 or TRIM7 isoform 4.

484 **(B-C)** HeLa-CD300lf cells expressing indicated constructs infected an multiplicity of

485 infection (MOI) of 50 with MNoV^{CW3} **(B)** or MNoV^{CR6} **(C)**. Cellular viability was assessed

486 72 hours post infection (hpi). Values are normalized for each cell line to uninfected

487 control wells to determine % viability. Data are shown as means ± SEM from three

488 independent experiments and data were analyzed by one-way ANOVA with Tukey's

489 multiple comparison test **p<0.01, ***p<0.001, ns = not significant.

490 **(D-E)** BV2 cells expressing indicated constructs infected an multiplicity of infection

491 (MOI) of 5 with MNoV^{CW3} **(D)** or MNoV^{CR6} **(E)**. Cellular viability was assessed 24 hours

492 post infection (hpi). Values are normalized for each cell line to uninfected control wells

493 to determine % viability. Data are shown as means ± SEM from three independent

494 experiments and data were analyzed by one-way ANOVA with Tukey's multiple

495 comparison test ***p<0.001, ****p<0.0001, ns = not significant.

496 **(F-G)** HeLa-CD300lf cells expressing indicated constructs infected an multiplicity of

497 infection (MOI) of 0.05 with MNoV^{CW3} **(F)** or MNoV^{CR6} **(G)**. Viral production was

498 assessed 24 hpi as measured by plaque assay. Data are shown as means ± SEM from

499 three independent experiments and data were analyzed by one-way ANOVA with

500 Tukey's multiple comparison test. ****p<0.0001, ns = not significant.

28

501   **(H-I)** BV2 cells expressing indicated constructs infected an multiplicity of infection (MOI)

502   of 0.05 with MNoV^{CW3} **(H)** or MNoV^{CR6} **(I)**.   Viral production was assessed 12 hpi as

503   measured by plaque assay. Data are shown as means ± SEM from three independent

504   experiments and data were analyzed by one-way ANOVA with Tukey's multiple

505   comparison test. ****$p<0.0001$, ns = not significant.

506   **(J)** BV2 expressing indicated constructs were transfected with viral RNA from MNoV^{CW3}

507   and harvested 12 hours post-transfection. Viral production was measured by plaque

508   assay. Data are shown as means ± SEM from three independent experiments and data

509   were analyzed by one-way ANOVA with Tukey's multiple comparison test.

510   ****$p<0.0001$, ns = not significant.

511

29

Gene Set Name	# Genes in Overlap (k)	p-value	FDR q-value
GO RESPONSE TO INTERFERON BETA	3	2.71E-08	1.62E-04
GO NEGATIVE REGULATION OF MULTI ORGANISM PROCESS	4	7.83E-08	2.33E-04
GO NEGATIVE REGULATION OF VIRAL GENOME REPLICATION	3	3.23E-07	6.43E-04
GO REGULATION OF VIRAL GENOME REPLICATION	3	1.18E-06	1.76E-03
GO NEGATIVE REGULATION OF VIRAL PROCESS	3	1.98E-06	2.36E-03
HALLMARK INTERFERON ALPHA RESPONSE	3	2.57E-06	2.55E-03
GO REGULATION OF MULTI ORGANISM PROCESS	4	7.18E-06	6.12E-03
GO DEFENSE RESPONSE TO VIRUS	3	1.24E-05	8.35E-03
GO NEGATIVE REGULATION OF VIRAL ENTRY INTO HOST CELL	2	1.26E-05	8.35E-03
GO RESPONSE TO INTERFERON ALPHA	2	1.40E-05	8.35E-03
HALLMARK INTERFERON GAMMA RESPONSE	3	2.25E-05	1.19E-02
GO REGULATION OF SYMBIOSIS ENCOMPASSING MUTUALISM THROUGH PARASITISM	3	2.42E-05	1.19E-02
GO PHOSPHATIDYLSERINE METABOLIC PROCESS	2	2.78E-05	1.19E-02
GO REGULATION OF VIRAL ENTRY INTO HOST CELL	2	2.78E-05	1.19E-02
GO CELLULAR MODIFIED AMINO ACID METABOLIC PROCESS	3	2.99E-05	1.19E-02
GO RESPONSE TO VIRUS	3	4.22E-05	1.53E-02
GO ALDITOL PHOSPHATE METABOLIC PROCESS	2	4.37E-05	1.53E-02
GO CELLULAR MODIFIED AMINO ACID BIOSYNTHETIC PROCESS	2	1.01E-04	3.35E-02

512

513 **Table 1: GSEA of BV2 CRISPRa screening hits**

514

30

Gene Set Name	# Genes in Overlap (k)	p-value	FDR q-value
GO NEGATIVE REGULATION OF RESPONSE TO STIMULUS	16	3.19E-12	1.90E-08
GO POSITIVE REGULATION OF BIOSYNTHETIC PROCESS	17	1.93E-11	5.76E-08
GO TRANSCRIPTION FROM RNA POLYMERASE II PROMOTER	12	5.05E-11	1.00E-07
GO POSITIVE REGULATION OF GENE EXPRESSION	16	1.15E-10	1.72E-07
GO RNA POLYMERASE II TRANSCRIPTION FACTOR ACTIVITY SEQUENCE SPECIFIC DNA BINDING	11	2.01E-10	2.40E-07
GO EMBRYO DEVELOPMENT	12	5.56E-10	5.53E-07
GO POSITIVE REGULATION OF MULTICELLULAR ORGANISMAL PROCESS	14	7.19E-10	5.66E-07
GO RESPONSE TO CYTOKINE	11	7.59E-10	5.66E-07
GO NEGATIVE REGULATION OF CELL COMMUNICATION	13	1.19E-09	7.90E-07
GO REGULATION OF TRANSCRIPTION FROM RNA POLYMERASE II PROMOTER	15	1.78E-09	9.76E-07
HALLMARK INTERFERON ALPHA RESPONSE	6	2.02E-09	9.76E-07
GO POSITIVE REGULATION OF TRANSCRIPTION FROM RNA POLYMERASE II PROMOTER	12	2.05E-09	9.76E-07
GO TISSUE DEVELOPMENT	14	2.13E-09	9.76E-07
GO SEQUENCE SPECIFIC DNA BINDING	12	2.94E-09	1.25E-06
GO NEGATIVE REGULATION OF VIRAL GENOME REPLICATION	5	3.73E-09	1.48E-06
GO TRANSCRIPTIONAL ACTIVATOR ACTIVITY RNA POLYMERASE II TRANSCRIPTION REGULATORY REGION SEQUENCE SPECIFIC BINDING	8	4.10E-09	1.53E-06
GO TRANSCRIPTION FACTOR ACTIVITY RNA POLYMERASE II CORE PROMOTER PROXIMAL REGION SEQUENCE SPECIFIC BINDING	8	5.62E-09	1.97E-06
GO TRANSCRIPTIONAL ACTIVATOR ACTIVITY RNA POLYMERASE II CORE PROMOTER PROXIMAL REGION SEQUENCE SPECIFIC BINDING	7	1.05E-08	3.49E-06
GO EPITHELIUM DEVELOPMENT	11	1.38E-08	4.18E-06
GO NUCLEIC ACID BINDING TRANSCRIPTION FACTOR ACTIVITY	12	1.47E-08	4.18E-06

515

516 **Table 2: GSEA of HeLa-CD300lf CRISPRa screening hits**

517

References:

518   **References:**

519   1.   Karst SM, Wobus CE, Goodfellow IG, Green KY, Virgin HW. Advances in norovirus biology. Cell
520   Host Microbe. 2014;15(6):668-80. doi: 10.1016/j.chom.2014.05.015. PubMed PMID: 24922570; PubMed
521   Central PMCID: PMCPMC4113907.
522   2.   Bartsch SM, Lopman BA, Hall AJ, Parashar UD, Lee BY. The potential economic value of a human
523   norovirus   vaccine   for   the   United   States.   Vaccine.   2012;30(49):7097-104.   doi:
524   10.1016/j.vaccine.2012.09.040. PubMed PMID: 23026689; PubMed Central PMCID: PMCPMC3517973.
525   3.   Ettayebi K, Crawford SE, Murakami K, Broughman JR, Karandikar U, Tenge VR, et al. Replication
526   of   human   noroviruses   in   stem   cell-derived   human   enteroids.   Science.   2016.   doi:
527   10.1126/science.aaf5211. PubMed PMID: 27562956.
528   4.   Jones MK, Watanabe M, Zhu S, Graves CL, Keyes LR, Grau KR, et al. Enteric bacteria promote
529   human   and   mouse   norovirus   infection   of   B   cells.   Science.   2014;346(6210):755-9.   doi:
530   10.1126/science.1257147. PubMed PMID: 25378626; PubMed Central PMCID: PMCPMC4401463.
531   5.   Orchard RC, Wilen CB, Doench JG, Baldridge MT, McCune BT, Lee YC, et al. Discovery of a
532   proteinaceous   cellular   receptor   for   a   norovirus.   Science.   2016;353(6302):933-6.   doi:
533   10.1126/science.aaf1220. PubMed PMID: 27540007.
534   6.   Haga K, Fujimoto A, Takai-Todaka R, Miki M, Doan YH, Murakami K, et al. Functional receptor
535   molecules CD300lf and CD300ld within the CD300 family enable murine noroviruses to infect cells. Proc
536   Natl Acad Sci U S A. 2016;113(41):E6248-E55. Epub 2016/09/28. doi: 10.1073/pnas.1605575113.
537   PubMed PMID: 27681626; PubMed Central PMCID: PMCPMC5068309.
538   7.   Park RJ, Wang T, Koundakjian D, Hultquist JF, Lamothe-Molina P, Monel B, et al. A genome-wide
539   CRISPR screen identifies a restricted set of HIV host dependency factors. Nat Genet. 2017;49(2):193-203.
540   Epub 2016/12/19. doi: 10.1038/ng.3741. PubMed PMID: 27992415; PubMed Central PMCID:
541   PMCPMC5511375.
542   8.   Zhang R, Miner JJ, Gorman MJ, Rausch K, Ramage H, White JP, et al. A CRISPR screen defines a
543   signal peptide processing pathway required by flaviviruses. Nature. 2016;535(7610):164-8. Epub
544   2016/06/17. doi: 10.1038/nature18625. PubMed PMID: 27383988; PubMed Central PMCID:
545   PMCPMC4945490.
546   9.   Ding S, Diep J, Feng N, Ren L, Li B, Ooi YS, et al. STAG2 deficiency induces interferon responses
547   via cGAS-STING pathway and restricts virus infection. Nat Commun. 2018;9(1):1485. Epub 2018/04/16.
548   doi: 10.1038/s41467-018-03782-z.   PubMed   PMID: 29662124;   PubMed   Central   PMCID:
549   PMCPMC5902600.
550   10.   Han J, Perez JT, Chen C, Li Y, Benitez A, Kandasamy M, et al. Genome-wide CRISPR/Cas9 Screen
551   Identifies Host Factors Essential for Influenza Virus Replication. Cell Rep. 2018;23(2):596-607. doi:
552   10.1016/j.celrep.2018.03.045. PubMed PMID: 29642015.
553   11.   Marceau CD, Puschnik AS, Majzoub K, Ooi YS, Brewer SM, Fuchs G, et al. Genetic dissection of
554   Flaviviridae host factors through genome-scale CRISPR screens. Nature. 2016;535(7610):159-63. Epub
555   2016/06/17. doi: 10.1038/nature18631. PubMed PMID: 27383987; PubMed Central PMCID:
556   PMCPMC4964798.
557   12.   Gilbert LA, Larson MH, Morsut L, Liu Z, Brar GA, Torres SE, et al. CRISPR-mediated modular RNA-
558   guided regulation of transcription in eukaryotes. Cell. 2013;154(2):442-51. Epub 2013/07/11. doi:
559   10.1016/j.cell.2013.06.044. PubMed PMID: 23849981; PubMed Central PMCID: PMCPMC3770145.
560   13.   Gilbert LA, Horlbeck MA, Adamson B, Villalta JE, Chen Y, Whitehead EH, et al. Genome-Scale
561   CRISPR-Mediated Control of Gene Repression and Activation. Cell. 2014;159(3):647-61. Epub
562   2014/10/09. doi: 10.1016/j.cell.2014.09.029. PubMed PMID: 25307932; PubMed Central PMCID:
563   PMCPMC4253859.

564   14.   Konermann S, Brigham MD, Trevino AE, Joung J, Abudayyeh OO, Barcena C, et al. Genome-scale
565   transcriptional activation by an engineered CRISPR-Cas9 complex. Nature. 2015;517(7536):583-8. Epub
566   2014/12/10. doi: 10.1038/nature14136. PubMed PMID: 25494202; PubMed Central PMCID:
567   PMCPMC4420636.
568   15.   Nice TJ, Strong DW, McCune BT, Pohl CS, Virgin HW. A single-amino-acid change in murine
569   norovirus NS1/2 is sufficient for colonic tropism and persistence. J Virol. 2013;87(1):327-34. doi:
570   10.1128/JVI.01864-12. PubMed PMID: 23077309; PubMed Central PMCID: PMCPMC3536416.
571   16.   Strong DW, Thackray LB, Smith TJ, Virgin HW. Protruding domain of capsid protein is necessary
572   and sufficient to determine murine norovirus replication and pathogenesis in vivo. J Virol.
573   2012;86(6):2950-8. doi: 10.1128/JVI.07038-11. PubMed PMID: 22258242; PubMed Central PMCID:
574   PMCPMC3302348.
575   17.   Wilen CB, Lee S, Hsieh LL, Orchard RC, Desai C, Hykes BL, et al. Tropism for tuft cells determines
576   immune   promotion   of   norovirus   pathogenesis.   Science.   2018;360(6385):204-8.   doi:
577   10.1126/science.aar3799. PubMed PMID: 29650672.
578   18.   Nice TJ, Baldridge MT, McCune BT, Norman JM, Lazear HM, Artyomov M, et al. Interferon-λ
579   cures   persistent   murine   norovirus   infection   in   the   absence   of   adaptive   immunity.   Science.
580   2015;347(6219):269-73. doi: 10.1126/science.1258100. PubMed PMID: 25431489; PubMed Central
581   PMCID: PMCPMC4398891.
582   19.   Nice TJ, Osborne LC, Tomov VT, Artis D, Wherry EJ, Virgin HW. Type I Interferon Receptor
583   Deficiency in Dendritic Cells Facilitates Systemic Murine Norovirus Persistence Despite Enhanced
584   Adaptive Immunity. PLoS Pathog. 2016;12(6):e1005684. doi: 10.1371/journal.ppat.1005684. PubMed
585   PMID: 27327515; PubMed Central PMCID: PMCPMC4915689.
586   20.   Baldridge MT, Nice TJ, McCune BT, Yokoyama CC, Kambal A, Wheadon M, et al. Commensal
587   microbes and interferon-λ determine persistence of enteric murine norovirus infection. Science.
588   2015;347(6219):266-9. doi: 10.1126/science.1258025. PubMed PMID: 25431490; PubMed Central
589   PMCID: PMCPMC4409937.
590   21.   Karst SM, Wobus CE, Lay M, Davidson J, Virgin HW. STAT1-dependent innate immunity to a
591   Norwalk-like virus. Science. 2003;299(5612):1575-8. doi: 10.1126/science.1077905. PubMed PMID:
592   12624267.
593   22.   Cadwell K, Patel KK, Maloney NS, Liu TC, Ng AC, Storer CE, et al. Virus-plus-susceptibility gene
594   interaction determines Crohn's disease gene Atg16L1 phenotypes in intestine. Cell. 2010;141(7):1135-
595   45.   doi: 10.1016/j.cell.2010.05.009.   PubMed   PMID: 20602997;   PubMed   Central   PMCID:
596   PMCPMC2908380.
597   23.   Kernbauer E, Ding Y, Cadwell K. An enteric virus can replace the beneficial function of
598   commensal   bacteria.   Nature.   2014;516(7529):94-8.   doi: 10.1038/nature13960.   PubMed   PMID:
599   25409145; PubMed Central PMCID: PMCPMC4257755.
600   24.   Doench JG, Fusi N, Sullender M, Hegde M, Vaimberg EW, Donovan KF, et al. Optimized sgRNA
601   design   to   maximize   activity   and   minimize   off-target   effects   of   CRISPR-Cas9.   Nat   Biotechnol.
602   2016;34(2):184-91. Epub 2016/01/18. doi: 10.1038/nbt.3437. PubMed PMID: 26780180; PubMed
603   Central PMCID: PMCPMC4744125.
604   25.   Liberzon A, Subramanian A, Pinchback R, Thorvaldsdóttir H, Tamayo P, Mesirov JP. Molecular
605   signatures   database   (MSigDB)   3.0.   Bioinformatics.   2011;27(12):1739-40.   Epub   2011/05/05.   doi:
606   10.1093/bioinformatics/btr260. PubMed PMID: 21546393; PubMed Central PMCID: PMCPMC3106198.
607   26.   Subramanian A, Tamayo P, Mootha VK, Mukherjee S, Ebert BL, Gillette MA, et al. Gene set
608   enrichment analysis: a knowledge-based approach for interpreting genome-wide expression profiles.
609   Proc Natl Acad Sci U S A. 2005;102(43):15545-50. Epub 2005/09/30. doi: 10.1073/pnas.0506580102.
610   PubMed PMID: 16199517; PubMed Central PMCID: PMCPMC1239896.

611   27.   Biering SB, Choi J, Halstrom RA, Brown HM, Beatty WL, Lee S, et al. Viral Replication Complexes
612   Are Targeted by LC3-Guided Interferon-Inducible GTPases. Cell Host Microbe. 2017;22(1):74-85.e7. Epub
613   2017/06/29. doi: 10.1016/j.chom.2017.06.005. PubMed PMID: 28669671.
614   28.   Skurat AV, Dietrich AD, Zhai L, Roach PJ. GNIP, a novel protein that binds and activates
615   glycogenin, the self-glucosylating initiator of glycogen biosynthesis. J Biol Chem. 2002;277(22):19331-8.
616   Epub 2002/03/26. doi: 10.1074/jbc.M201190200. PubMed PMID: 11916970.
617   29.   Chakraborty A, Diefenbacher ME, Mylona A, Kassel O, Behrens A. The E3 ubiquitin ligase Trim7
618   mediates c-Jun/AP-1 activation by Ras signalling. Nat Commun. 2015;6:6782. Epub 2015/04/08. doi:
619   10.1038/ncomms7782. PubMed PMID: 25851810; PubMed Central PMCID: PMCPMC4395875.
620   30.   Montori-Grau M, Pedreira-Casahuga R, Boyer-Díaz Z, Lassot I, García-Martínez C, Orozco A, et al.
621   GNIP1 E3 ubiquitin ligase is a novel player in regulating glycogen metabolism in skeletal muscle.
622   Metabolism. 2018. Epub 2018/02/18. doi: 10.1016/j.metabol.2018.02.005. PubMed PMID: 29466708.
623   31.   Doench JG. Am I ready for CRISPR? A user's guide to genetic screens. Nat Rev Genet.
624   2018;19(2):67-80. Epub 2017/12/04. doi: 10.1038/nrg.2017.97. PubMed PMID: 29199283.
625   32.   Yau R, Rape M. The increasing complexity of the ubiquitin code. Nat Cell Biol. 2016;18(6):579-86.
626   doi: 10.1038/ncb3358. PubMed PMID: 27230526.
627   33.   Esposito D, Koliopoulos MG, Rittinger K. Structural determinants of TRIM protein function.
628   Biochem Soc Trans. 2017;45(1):183-91. doi: 10.1042/BST20160325. PubMed PMID: 28202672.
629   34.   Hwang S, Alhatlani B, Arias A, Caddy SL, Christodoulou C, Cunha JB, et al. Murine norovirus:
630   propagation, quantification, and genetic manipulation. Curr Protoc Microbiol. 2014;33:15K.2.1-61. Epub
631   2014/05/01. doi: 10.1002/9780471729259.mc15k02s33. PubMed PMID: 24789596; PubMed Central
632   PMCID: PMCPMC4074558.

633

634

635 **Supporting Information Legends**

636 **Supplemental Methods:** DNA sequences used for this study

637 **Table S1:** STARS analysis of CRISPRa screen in BV2 cells for MNoV^{CW3}

638 **Table S2:** STARS analysis of CRISPRa screen in BV2 cells for MNoV^{CR6}

639 **Table S3:** STARS analysis of CRISPRa screen in HeLa-CD300lf cells for MNoV^{CW3}

640 **Table S4:** STARS analysis of CRISPRa screen in HeLa-CD300lf cells for MNoV^{CR6}

641